Nonlinear coupling of relative intensity noise from pump to a fiber ring laser mode-locked with carbon nanotubes

Kan Wu,[1,*] Jia Haur Wong,[1] Ping Shum,[1] Songnian Fu,[1] Chunmei Ouyang,[1] Honghai Wang,[1] E. J. R. Kelleher,[2] A. I. Chernov,[3] E. D. Obraztsova[3] and Jianping Chen[4]

[1]*School of Electrical & Electronic Engineering, Nanyang Technological University, 637553 Singapore*
[2]*Femtosecond Optics Group, Physics Department, Imperial College London, London SW7 2AZ, UK*
[3]*A.M. Prokhorov General Physics Institute, Russian Academy of Science, 38 Vavilov Street, Moscow, 119991 Russia*
[4]*The State Key Laboratory on Advanced Optical Communication Systems and Networks, Shanghai Jiao Tong University, 200051 China*
**wuka0002@ntu.edu.sg*

Abstract: Pump relative intensity noise (RIN) has been recognized as a major source of noise in mode-locked lasers. The coupling of RIN from the pump to the output of a passively mode-locked fiber laser (PMFL) is systematically investigated using a pump modulation technique. It is found that the linear RIN coupling ratio from pump to PMFL is decreased with an increase in modulation frequency and is independent of modulation power. Moreover, the nonlinear RIN coupling from pump to PMFL is clearly demonstrated with a square wave modulated pump. The nonlinear RIN coupling ratio is noise power dependent. An exponential decay model based on the view of gain modulation is proposed and explains well the behavior of the nonlinear coupling phenomena.

OCIS codes: (140.3510) Lasers fiber; (140.4050) Mode-locked lasers; (120.3940) Metrology

References and links

1. J. J. McFerran, W. C. Swann, B. R. Washburn, and N. R. Newbury, "Elimination of pump-induced frequency jitter on fiber-laser frequency combs," Opt. Lett. **31**(13), 1997–1999 (2006).
2. G. C. Valley, "Photonic analog-to-digital converters," Opt. Express **15**(5), 1955–1982 (2007).
3. J. Kim, J. A. Cox, J. Chen, and F. X. Kartner, "Drift-free femtosecond timing synchronization of remote optical and microwave sources," Nat. Photonics **2**(12), 733–736 (2008).
4. D. Linde, "Characterization of the Noise in Continuously Operating Mode-Locked Lasers," Appl. Phys. B **39**(4), 201–217 (1986).
5. H. A. Haus, and A. Mecozzi, "Noise of mode-locked lasers," IEEE J. Quantum Electron. **29**(3), 983–996 (1993).
6. S. Namiki, and H. A. Haus, "Noise of the stretched pulse fiber laser. I. Theory," IEEE J. Quantum Electron. **33**(5), 649–659 (1997).
7. R. Paschotta, "Noise of mode-locked lasers (Part I): numerical model," Appl. Phys. B **79**(2), 153–162 (2004).
8. K. Wu, J. H. Wong, P. Shum, D. R. C. S. Lim, V. K. H. Wong, K. E. K. Lee, J. Chen, and E. D. Obraztsova, "Timing-jitter reduction of passively mode-locked fiber laser with a carbon nanotube saturable absorber by optimization of cavity loss," Opt. Lett. **35**(7), 1085–1087 (2010).
9. C. Ouyang, L. Chai, H. Zhao, M. Hu, Y. Song, and C. Wang, "Position Effect of Spectral Filter on Properties of Highly Chirped Pulses in an All-Normal-Dispersion Fiber Laser," IEEE J. Quantum Electron. **45**(10), 1284–1288 (2009).
10. N. Dogru, and M. S. Ozyazici, "Intensity noise of mode-locked fiber grating external cavity semiconductor lasers," Opt. Quantum Electron. **35**(2), 169–178 (2003).
11. W. Lee, M. T. Choi, H. Izadpanah, and R. J. Delfyett, "Relative intensity noise characteristics of frequency stabilised grating-coupled modelocked semiconductor laser," Electron. Lett. **42**(20), 1156–1157 (2006).
12. N. R. Newbury, and B. R. Washburn, "Theory of the frequency comb output from a femtosecond fiber laser," IEEE J. Quantum Electron. **41**(11), 1388–1402 (2005).
13. J. J. McFerran, W. C. Swann, B. R. Washburn, and N. R. Newbury, "Suppression of pump-induced frequency noise in fiber-laser frequency combs leading to sub-radian f (ceo) phase excursions," Appl. Phys. B **86**(2), 219–227 (2007).

#127700 - $15.00 USD Received 28 Apr 2010; revised 8 Jun 2010; accepted 15 Jun 2010; published 23 Jul 2010

14. B. R. Washburn, W. C. Swann, and N. R. Newbury, "Response dynamics of the frequency comb output from a femtosecond fiber laser," Opt. Express **13**(26), 10622–10633 (2005).
15. I. L. Budunoğlu, C. Ulgüdür, B. Oktem, and F. Ö. Ilday, "Intensity noise of mode-locked fiber lasers," Opt. Lett. **34**(16), 2516–2518 (2009).
16. J. Chen, J. W. Sickler, P. Fendel, E. P. Ippen, F. X. Kärtner, T. Wilken, R. Holzwarth, and T. W. Hänsch, "Generation of low-timing-jitter femtosecond pulse trains with 2 GHz repetition rate via external repetition rate multiplication," Opt. Lett. **33**(9), 959–961 (2008).
17. H. Tsuchida, "Correlation between amplitude and phase noise in a mode-locked Cr:LiSAF laser," Opt. Lett. **23**(21), 1686–1688 (1998).
18. S. Y. Set, H. Yaguchi, Y. Tanaka, M. Jablonski, Y. Sakakibara, A. Rozhin, M. Tokumoto, H. Kataura, Y. Achiba, and K. Kikuchi, "Mode-locked fiber lasers based on a saturable absorber incorporating carbon nanotubes," in *Optical Fiber Communications Conference, 2003. OFC 2003*, 2003), PD44–P41–43 vol.43.
19. A. V. Tausenev, E. D. Obraztsova, A. S. Lobach, A. I. Chernov, V. I. Konov, P. G. Kryukov, A. V. Konyashchenko, and E. M. Dianov, "177 fs erbium-doped fiber laser mode locked with a cellulose polymer film containing single-wall carbon nanotubes," Appl. Phys. Lett. **92**(17), 171113 (2008).
20. E. J. R. Kelleher, J. C. Travers, Z. Sun, A. G. Rozhin, A. C. Ferrari, S. V. Popov, and J. R. Taylor, "Nanosecond-pulse fiber lasers mode-locked with nanotubes," Appl. Phys. Lett. **95**(11), 111108 (2009).
21. T. Hasan, Z. P. Sun, F. Q. Wang, F. Bonaccorso, P. H. Tan, A. G. Rozhin, and A. C. Ferrari, "Nanotube-Polymer Composites for Ultrafast Photonics," Adv. Mater. **21**(38â€"39), 3874–3899 (2009).
22. S. Yamashita, Y. Inoue, K. Hsu, T. Kotake, H. Yaguchi, D. Tanaka, M. Jablonski, and S. Y. Set, "5-GHz pulsed fiber Fabry-Pe/spl acute/rot laser mode-locked using carbon nanotubes," IEEE Photon. Technol. Lett. **17**(4), 750–752 (2005).
23. A. I. Chernov, E. D. Obraztsova, and A. S. Lobach, "Optical properties of polymer films with embedded single-wall carbon nanotubes," Phys. Status Solidi **244**(11), 4231–4235 (2007).
24. P. A. Obraztsov, A. A. Sirotkin, E. D. Obraztsova, Y. P. Svirko, and S. V. Garnov, "Carbon-nanotube-based saturable absorbers for near infrared solid state lasers," Opt. Rev. **17**(3), 290 (2010).
25. G. P. Agrawal, Applications of Nonlinear Fiber Optics, (2001).

1. Introduction

Low noise mode-locked fiber lasers are compact and economical sources for frequency metrology [1], optical analog-digital conversion [2] and drift-free optical timing distribution [3]. The dynamics of mode-locked lasers has been widely investigated [4–9]. Properties of the relative intensity noise (RIN) have also been discussed by many researchers [10–15]. Dogru first proposed a theoretical model of RIN in a mode-locked hybrid soliton laser where a chirped fiber Bragg grating (CFBG) was used as a reflection mirror [10]. Lee experimentally examined the RIN characteristics of a frequency stabilized grating-coupled mode-locked semiconductor laser [11]. Recently, Newbury and his colleagues McFerran, Washburn and Swann have reported a series of analytical and experimental studies on noise in fiber-laser based frequency combs [12–14]. Budunoglu also discussed the RIN of mode-locked fiber lasers with respect to different cavity dispersions maps [15].

Due to the noise coupled from the electrical circuits, the pump laser has been identified as a major source of noise in passively mode-locked fiber lasers (PMFLs). It has been reported that the RIN coupling from pump to laser can significantly deteriorate the noise performance of PMFLs [16]. However, the behavior of this coupling is still unclear and only a simple point-to-point mapping model with a knee frequency is usually used to explain it [13]. This model is described in Eq. (1), where ε is the coupling ratio and f_{knee} is the knee frequency. The pump RIN at frequency f_0 will couple to the laser RIN at the same frequency with coefficient $\varepsilon(1+(f_0 / f_{knee})^2)^{-1}$ and the laser RIN at other frequency will not be affected. In the following part of this paper, we call this linear noise coupling. This model is simple and easy for analysis but the validity and accuracy of this model have not been explicitly proven.

$$RIN_{laser}(f) = \frac{\varepsilon}{1+(f / f_{knee})^2} RIN_{pump}(f) \tag{1}$$

In this paper, we investigate this coupling effect by modulating the drive current of the pump diode, which has been verified as an effective method to study the RIN coupling phenomena [17]. We try to answer four questions: (i) Does the laser have the same coupling ratio at all noise frequencies from the pump RIN? (ii) How does the laser respond to the same frequency noise with different noise power? (iii) Is the RIN coupling from pump to laser a

#127700 - $15.00 USD Received 28 Apr 2010; revised 8 Jun 2010; accepted 15 Jun 2010; published 23 Jul 2010

linear point-to-point mapping process or a nonlinear point-to-multipoint mapping process? (iv) If the coupling is nonlinear, how does it behave and why does it behave like this?

2. Experiment

Single wall carbon nanotubes (SWCNTs) have been recently emerged as a versatile saturable absorber device for PMFLs [18–23]. The PMFL under study is shown in Fig. 1. The SWCNTs used as saturable absorbers for mode locking operation are integrated into the cavity on the end of the fiber connector, as shown in the inset of Fig. 1. The individual SWCNTs are embedded in carboximethyl cellulose (CMC) film with special treatment [23]. Such composite provides a high damage threshold and low pump power for a self-started mode locking [19]. The transmittance at low optical power is ~39% and the saturable absorption is 12%~15% of the total loss. The relaxation time is ~300fs [24]. A hybrid component Tap/Isolator/WDM (Opneti TIWDM-98-D-10-B-L-10-FC) integrating the functionalities of tap output (10%), isolator and 980/1550 WDM is utilized to simplify the cavity structure. The total cavity length is ~3.4 m and the corresponding fundamental repetition rate is ~58.7 MHz The length of the single mode fiber is ~2.8 m with a dispersion of −0.022 ps^2/m. The length of Erbium doped fiber (LIEKKI Er110) is ~0.6 m with a dispersion of 0.012 ps^2/m. Thus the total dispersion is ~-0.054 ps^2. The drive current of the pump (DC bias current in Fig. 1) is 170.1 mA, corresponding to a pump power of 67mW. The output power is −3.1dBm and the 3-dB spectral width is 6.6nm. The mode locking at fundamental repetition frequency can be achieved at the pump power of 52 mW to 78 mW. Modulation current (AC modulation current in Fig. 1) is applied to the 976 nm pump diode to simulate the pump RIN. A signal source analyzer (SSA, Rohde & Schwarz FSUP26) is used to measure the RIN spectrum of the laser output after optical-electrical conversion by a 2 GHz photo detector. To maintain the laser operation, the modulation current is adjusted from 1 mA to 6 mA, corresponding to 0.6~3.5% power fluctuation of the pump diode. The pump RIN is measured with the baseband noise measurement module of the SSA.

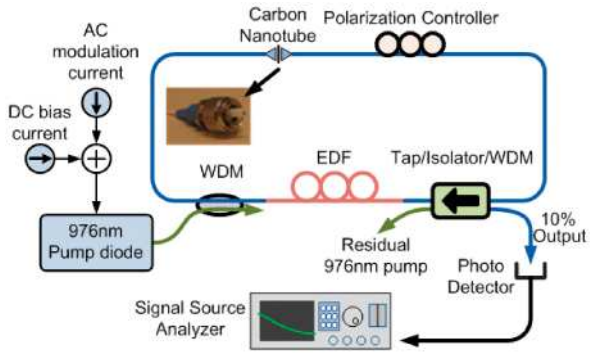

Fig. 1. Experimental setup of passively mode-locked fiber ring laser and pump modulation.

We first investigate the frequency response of the laser by modulating a sine wave to the pump bias current with different frequencies f_{mod}. Due to the nonlinear response of the pump diode output with respect to the modulation signal, a given modulation current will generate a slightly different peak power at each f_{mod} and some harmonics of f_{mod} are generated. Therefore the pump noise generated by current modulation is a frequency comb noise, rather than a single frequency noise. The modulation frequency is experimentally varied from 2.5 kHz to 80 kHz with the modulation current fixed at 6 mA.

The RIN measurement results of the pump and the PMFL at 2.5 kHz and 20 kHz modulation are shown in Fig. 2(a). It can be seen that different peak values are present for different f_{mod} in the pump RIN spectra, together with harmonic generation, which verify the nonlinear response of the pump diode. Strong harmonics can be observed in the PMFL RIN

#127700 - $15.00 USD Received 28 Apr 2010; revised 8 Jun 2010; accepted 15 Jun 2010; published 23 Jul 2010

spectra both for $f_{\mathrm{mod}} = 2.5kHz$ and $f_{\mathrm{mod}} = 20kHz$, which suggests a nonlinear enhancement of the harmonics.

We define the total RIN coupling ratio as $C_{Tot}(f, P_p) = P_l(f, P_p) / P_p(f)$ where $P_l(f, P_p)$ and $P_p(f)$ are the values of RIN spectra of the PMFL and pump at frequency f. The total RIN coupling ratio is the combined effect of the linear coupling ratio $C_{Lin}(f)$ and the nonlinear coupling ratio $T_{Nonlin}(f, P_p)$. The linear coupling ratio $C_{Lin}(f) = \tilde{P}_l(f) / P_p(f)$ is noise power independent, where $\tilde{P}_l(f)$ is the component of noise power in the laser from linear coupling. The nonlinear coupling ratio $T_{Nonlin}(f, P_p)$ is noise power dependent. The total RIN coupling ratio at each harmonic frequency kf_{mod} is summarized in Fig. 2(b) for various values of f_{mod}. It can be observed that the RIN coupling ratio at a given frequency differs for varying harmonic orders, e.g. the 2nd harmonic frequency in the 2.5 kHz curve and the fundamental frequency in the 5 kHz curve have different total RIN coupling ratio. Thus, we can conclude that nonlinear coupling exists together with linear coupling.

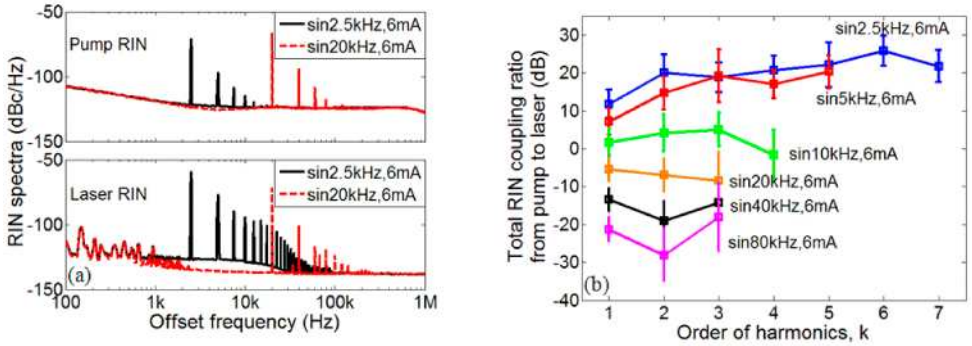

Fig. 2. (a) RIN spectra of the pump and the laser when different modulation frequencies are applied to the pump; (b) Total RIN coupling ratio from pump to laser for different modulation frequencies and their harmonics

To investigate the linear RIN coupling and the nonlinear RIN coupling separately, we measure the total coupling ratio at 5 kHz sine wave modulation with different modulation currents, as shown in Fig. 3(a). It can be seen that $C_{Tot}(f, P_p)$ at f_{mod} (i.e., k = 1) is independent of noise power (modulation current) and thus $C_{Tot}(f_{\mathrm{mod}}, P_p) = C_{Lin}(f_{\mathrm{mod}})$ and therefore the linear RIN coupling ratio $C_{Lin}(f_{\mathrm{mod}})$ can be obtained based on the data from Fig. 2(b) (values for k = 1 in each curve) and is summarized in Fig. 3(b). It is clearly observed that the linear coupling ratio decreases with the modulation frequency. For the frequency region in which the linear coupling ratio is greater than 0 dB, e.g. $f_{\mathrm{mod}} \le 10kHz$, the laser RIN generated by pump modulation is even stronger than the pump RIN, which is probably due to the fact that the low modulation frequency is closer to the EDF response time (~ms) and thus causes a stronger perturbation to the laser operation than high modulation frequency does [14]. This can also be demonstrated by the observation that the laser RIN spectrum (the baseline, not the frequency spurs) in Fig. 2(a) is higher at offset frequencies of 100 Hz~30 kHz under 2.5 kHz pump modulation. When we further increase the modulation frequency to 1 kHz, even with very small modulation depth, the laser is strongly disturbed and the mode locked state will disappear easily.

Square wave modulation is applied to further demonstrate the nonlinear coupling in the PMFL. For an ideal square wave with 50% duty-cycle, the power of even order harmonics is naturally suppressed. A typical pump RIN spectrum for 5 kHz square wave modulation is given in Fig. 4(a). The ~5dB steps at 100 kHz and 300 kHz offset frequencies are due to the

#127700 - $15.00 USD Received 28 Apr 2010; revised 8 Jun 2010; accepted 15 Jun 2010; published 23 Jul 2010

finite resolution of the SSA, which can only be set to 300 Hz in the range of 100 kHz~300 kHz. It can be clearly observed that the power of even order harmonics is suppressed by ~30 dB as compared to the adjacent odd order harmonics in the pump RIN. However, after coupling to the laser RIN spectrum in Fig. 4(a), the power of even order harmonics has been significantly enhanced. The total RIN coupling ratio with different modulation currents is summarized in Fig. 4(b). The high total coupling ratio for even order harmonics further confirms the nonlinear coupling of RIN. For low modulation current, e.g., 1 mA, (corresponding to low noise power), the total RIN coupling ratio is very similar to the linear RIN coupling ratio in Fig. 3(b).

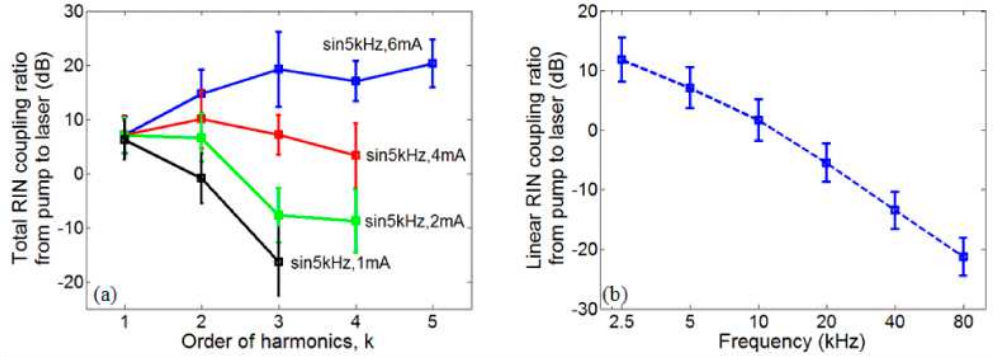

Fig. 3. (a) Total RIN coupling ratio from pump to laser at 5 kHz modulation for different modulation currents; (b) Linear RIN coupling ratio from pump to laser for different modulation frequencies

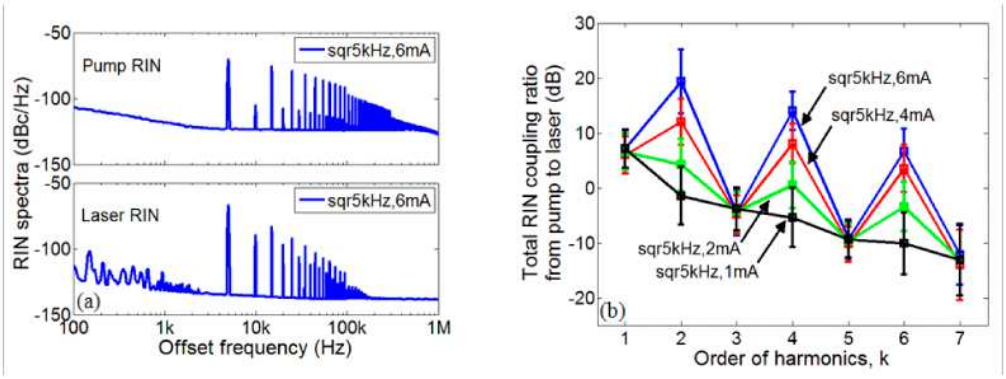

Fig. 4. (a) RIN spectra of pump and laser when square wave modulation is applied to the pump; (b) Total RIN coupling ratio from pump to laser with respect to different modulation current in a square wave modulation

3. Model and physical explanation

Here we propose an exponential decay model in order to describe the nonlinear RIN coupling from pump to PMFL. We only consider the nonlinearity generated by the fundamental frequency in our model, while the effects of harmonics are neglected due to their lower power. The effect of pump RIN on PMFL RIN can be described with Eq. (2) where $k = 2, 3, 4...$ is the order of the harmonic frequency, $C_{lin}(kf_{\mathrm{mod}})$ is the linear coupling ratio as depicted in Fig. 3(b), $T_{nonlin}(k)$ is the nonlinear coupling ratio from the fundamental frequency f_{mod} to its harmonic frequency kf_{mod}. We then express C_{lin} with a Lorentz shape [13] (the coefficient in Eq. (1)) and T_{nonlin} with an exponential decay model in Eq. (3), where

#127700 - $15.00 USD Received 28 Apr 2010; revised 8 Jun 2010; accepted 15 Jun 2010; published 23 Jul 2010

η and α represent the basic coupling ratio and attenuation speed of the coupling, respectively. T_{nonlin} can be obtained by subtracting the contribution of linear coupling in the laser RIN. Figure 5(a) gives the residual RIN contributed from nonlinear coupling and the values of η and α can be obtained by linear fit of each curve. The slope of the square-wave-modulation curves is smaller than that of the sine-wave-modulation curves because the power contained in the harmonics of the former is much higher than in the latter, resulting in greater nonlinear coupling from harmonics in the former. The fitting of the exponential decay model (dashed lines) based on Eq. (2) and Eq. (3) is shown in Fig. 5(b), which agrees well with the experimental data (solid lines). If the power at f_{mod} is low, the nonlinear RIN coupling term in Eq. (2) is then negligible and the coupling becomes a well-known linear point-to-point mapping process with a knee frequency f_{knee} in Eq. (1) [13]. The extracted values of η and α are listed in Table 1.

$$\begin{aligned} RIN_l(kf_{\mathrm{mod}}) &= C_{Tot} \cdot RIN_p(kf_{\mathrm{mod}}) \\ &= C_{Lin} RIN_p(kf_{\mathrm{mod}}) + T_{Nonlin}(k) RIN_p(f_{\mathrm{mod}}) \end{aligned} \tag{2}$$

$$T_{Nonlin}(k) = \eta e^{-\alpha k} \tag{3}$$

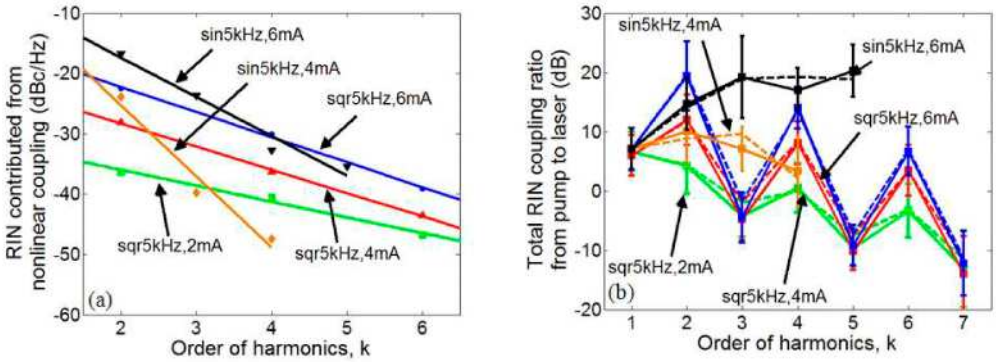

Fig. 5. (a) Residual RIN contributed from nonlinear coupling. Markers are experimental data; solid lines are linear fit; (b) Fitting of exponential decay model (dashed lines) of total RIN coupling ratio from pump to laser based on Eq. (2) and Eq. (3), and the experimental data (solid lines) of coupling ratio

Table 1. Values of η and α under different modulation waveform and modulation depth

Modulation	*sin5kHz,6mA*	*sin5kHz,4mA*	*sqr5kHz,6mA*	*sqr5kHz,4mA*	*sqr5kHz,2mA*
η	1.94	3.51	0.213	0.0459	0.00438
α	1.50	2.71	0.957	0.886	0.601

Here we give an explanation of the physical basis of nonlinear noise coupling phenomenon. For a three-level pumping scheme, the gain coefficient can be given by $g = \sigma(N_2 - N_1)$, where σ is the transition cross section and N_2 and N_1 are the atomic densities in the two energy states [25]. A weak modulation of pump can be modeled as a linear modulation of $g = g_0(1 + \varepsilon \sin \omega_0 t)$, where g_0 is the gain coefficient without pump modulation, ε is the modulation depth and $f_0 = \omega_0 / 2\pi$ is the modulation frequency. Then, for the ease of discussion, the total gain for an EDF can be given by Eq. (4), where gain fluctuation ΔG can be further expanded in Eq. (5). Therefore, it can be clearly seen that nonlinear terms exist. The direct calculation of the coefficient of frequency components at

#127700 - $15.00 USD Received 28 Apr 2010; revised 8 Jun 2010; accepted 15 Jun 2010; published 23 Jul 2010

ω_0, $2\omega_0$ and etc. is not very easy because, for example, $\sin^3 \omega_0 t$ will also generate $\sin \omega_0 t$ term as well as $\sin 3\omega_0 t$ term. Numerically, Fourier series will help to determine the values of these coefficients. The calculated coefficients are plotted in Fig. 6 when the modulation depth ε varies from 0.01 to 0.1. Note that the modulation depth of pump modulation is 0.006~0.035 in our experiment. The vertical axis is plotted in logarithm scale. These coefficients show very good linearity and verify the validity of the exponential decay model we have proposed in Eq. (3). Compared with the data of sine wave modulation in Fig. 5(a), the behaviors of curves at different modulation depth in Fig. 6 are very similar. For sine wave modulation, basic coupling ratio η is mainly determined by the gain fiber properties and is nearly unchanged with the modulation depth ε. Attenuation speed α will inversely increase with the decrease of modulation depth ε. For square wave modulation, the mechanism is the same. However the power of odd order harmonics is high enough to cause additional nonlinear coupling. A commonly used solution is to calculate the noise coupling at each harmonic frequency independently and summate them together. Instead, we can also use an exponential decay model to fit the data at even order frequency components. The fitting results in Fig. 5(b) have demonstrated the accuracy of this simplified fitting solution.

$$G = \exp(g) = \exp(g_0 + \Delta g) = G_0(1 + \Delta G) \tag{4}$$

$$\Delta G = \exp(\varepsilon \sin \omega_0 t) - 1 = \varepsilon \sin \omega_0 t + \frac{1}{2}(\varepsilon \sin \omega_0 t)^2 + \frac{1}{6}(\varepsilon \sin \omega_0 t)^3 + \ldots \tag{5}$$

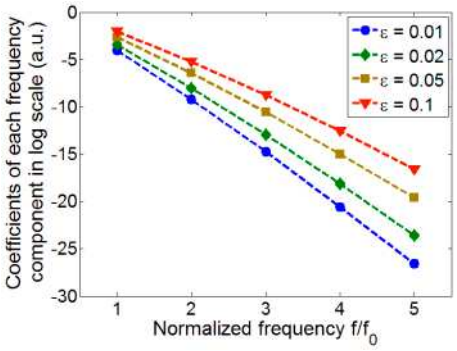

Fig. 6. Coefficients of each frequency component based on Eq. (5) at different modulation depth ε. The vertical axis is plotted in logarithm scale. The coefficients show very good linearity which verifies the validity of the exponential decay model we have proposed in Eq. (3).

4. Discussion

From the theoretical analysis above, we also notice that this nonlinear noise coupling phenomenon is due to the properties of gain medium. This means the nonlinear noise coupling we have observed in the fiber laser mode locked with carbon nanotubes can be applied to the mode-locked lasers with other mechanisms. We experimentally show the existence of nonlinear noise coupling in a passively mode-locked fiber laser based on nonlinear polarization rotation (NPR). The square wave modulation is applied and the results are shown in Fig. 7. The bias current of the pump is 238.7mA, corresponding to the pump power of ~103mW. The modulation current is 1mA and the modulation depth is therefore 0.4%. The modulation depth is very small compared with the values used in the CNT based mode-locked laser because the NPR mode locking is very sensitive to the pulse power and the fluctuation of gain will significantly affect the NPR mode locking operation. The offset frequency range in Fig. 7 is set from 1kHz to 30kHz because the modulation depth is very small and the laser RIN noise spurs after 30kHz are too weak to be characterized. In Fig. 7, the values of the

#127700 - $15.00 USD Received 28 Apr 2010; revised 8 Jun 2010; accepted 15 Jun 2010; published 23 Jul 2010

pump RIN at even order harmonic frequencies are ~30dB smaller than their adjacent odd order harmonic frequencies. However the difference of the NPR laser RIN values between even order and adjacent odd order frequencies is less than 15dB, which clearly demonstrates the existence of nonlinear noise coupling.

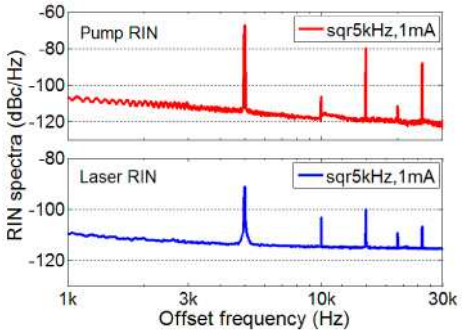

Fig. 7. RIN spectra of pump and NPR laser when square wave modulation is applied to the pump. The offset frequency range is set from 1kHz to 30kHz because the modulation depth is very small and laser RIN noise spurs after 30kHz are too small to be characterized.

Our theoretical and experimental results show that a periodic noise coupled from the pump source will not only generate a periodic noise with same frequency in the intensity noise of mode-locked laser, but will also generate serials of harmonic frequency noise. and therefore the intensity noise of the mode-locked laser will be significantly deteriorated and not easy to be managed. Definitely, the nonlinear noise coupling will reduce the accuracy of frequency metrology, the effective number of bit in optical sampling and the timing precision in timing distribution system, etc. The source of the periodic noise can be from the noise in power line, the internal noise from the drive circuit and/or the noise coupled from the free space.

5. Conclusion

In conclusion, the nonlinear RIN coupling from pump to PMFL is investigated by the pump modulation technique. The linear RIN coupling ratio from pump to laser decreases with the increase of frequency and is independent of the noise power. The nonlinear RIN coupling generates additional noise power at various harmonics kf_{mod} with respect to the fundamental modulation frequency f_{mod}. The nonlinear coupling ratio is determined by the noise power at f_{mod}, and exponentially decreases with an increase in harmonic order. A square wave pump modulation clearly illustrates this nonlinear noise coupling phenomenon. An exponential decay model is proposed to describe the behavior of the nonlinear coupling. Physical explanation of the nonlinear noise coupling effect from the view of gain modulation is presented. The theoretical analysis demonstrates the existence of nonlinear noise coupling and verifies the validity of exponential decay model.

#127700 - $15.00 USD Received 28 Apr 2010; revised 8 Jun 2010; accepted 15 Jun 2010; published 23 Jul 2010